

Impact of the Higher-Order Noise Filtering on the Performance of the PID Controller and Dead-Time Compensating DTC-PID Controller

Aleksandar I. Ribić
Institute Mihajlo Pupin
Belgrade, Serbia
aleksandar.ribic@pupin.rs

Miroslav R. Mataušek
Faculty of Electrical Engineering, University of Belgrade
Belgrade, Serbia
matausek@etf.rs

Abstract— A recently proposed dead-time compensating DTC-PID controller is compared with the PID controller in the presence of the higher-order noise filtering. Simulation and experimental results confirm that in the presence of the fourth-order noise filtering the relative advantages of the DTC-PID controller are preserved, enabling the effective application of the derivative action in the presence of the high measurement noise.

Keywords- PID control; Measurement noise; Robustness

I. INTRODUCTION

The controller with derivative action is a prerequisite for obtaining high performance for lag dominated stable, integrating and unstable processes [1]. Significant improvement of the performance/robustness tradeoff is obtained by the Dead-Time Compensating antiwindup PID (DTC-PID) controller with the second-order noise filter [2], compared to the PID controller, both optimized under the same constraints on the sensitivity to measurement noise and robustness. However, the large variation of control signal, accelerating the wear of active elements in actuator, might be the consequence of aggressive tuning used to obtain the fast rejection of the load step disturbance. In this case the higher-order noise filtering must be applied when applying the derivative action.

In the present paper advantages of the DTC-PID controller over the PID controller, both with the higher-order noise filtering, are analyzed and confirmed by simulation and on the laboratory thermal plant with noisy measurements.

II. THE CONTROLLER OPTIMIZATION AND SIMULATION ANALYSIS

The DTC-PID controller is defined by parameters $q=\{a_0, a_1, a_2, T_i, L\}$, the transfer function

$$C(s, q) = -\frac{U(s)}{Y(s)} = \frac{a_2 s^2 + a_1 s + a_0}{(T_i s + 1)^n - e^{-Ls}}, \quad 2 \leq n, \quad (1)$$

relating the controlled variable $Y(s)$ to the control variable $U(s)$, for $w(t) \equiv u(t)$, and the implementation in Fig. 1.

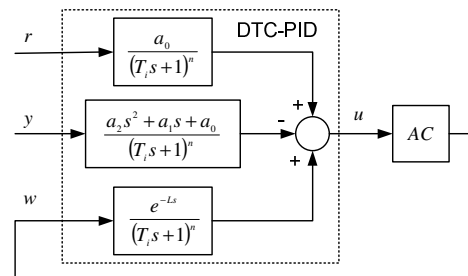


Figure 1. The antiwindup DTC-PID controller with the higher-order noise filter, $2 \leq n$. Signal y is the controlled variable. Manipulated variable w is the response of the actuator AC to the control signal u . The set-point is r .

The PID controller, with the transfer function relating $Y(s)$ to $U(s)$ given by $C(s, q) = (k_d s + k + k_i/s) / (T_i s + 1)^{n-1}$, $2 \leq n$, is defined by parameters $q = \{k, k_i, k_d, T_i\}$ and the following implementation

$$U(s) = k(bR(s) - Y_f(s)) + \frac{k_i}{s}(R(s) - Y_f(s)) - k_d s Y_f(s) \quad (2)$$

$$Y_f(s) = F_n(s)Y(s) \quad (3)$$

with $b=0$, if not stated otherwise, and with the noise filter $F_n(s)$ defined by

$$F_n(s) = \frac{1}{(T_i s + 1)^{n-1}}, \quad 2 \leq n. \quad (4)$$

The additional second-order noise filtering, applied in the DTC-PID controller from [2], corresponds to the additional second-order noise filtering, applied to the real PID controller with the first-order noise filter from [1]. This follows from the transfer functions $C(s, q)$ of both controllers. Namely, for $n=4$ in (1) and (4), and for $\exp(-Ls) \approx 1 - Ls$ in (1), one obtains denominator of the transfer function $C(s, q)$ given by: $D(s) = s\{(T_i)^4 s^3 + 4(T_i)^3 s^2 + 6(T_i)^2 s + 4T_i + L\}$ for DTC-PID controller while $D(s) = s\{(T_i)^3 s^3 + 3(T_i)^2 s^2 + 3(T_i)s + 1\}$ for the PID controller.

Robustness is defined by the maximum sensitivity M_S and maximum complementary sensitivity M_T , as

$$M_S = \max_{\omega} |S(i\omega, q)|, \quad M_T = \max_{\omega} |1 - S(i\omega, q)|, \quad (5)$$

where the sensitivity function $S(s, q)$ and the loop-transfer function $C_L(s, q)$ are given by

$$S(i\omega, q) = \frac{1}{1 + C_L(i\omega, q)}, \quad C_L(i\omega, q) = C(i\omega, q)G_p(i\omega). \quad (6)$$

The sensitivity to measurement noise, defined by the ratio of the standard deviations of the control signal σ_u and the measurement noise σ_n , is given by

$$M_n = \frac{\sigma_u}{\sigma_n} = \sqrt{\frac{1}{\omega_c} \int_0^{\omega_c} C_u(i\omega, q)C_u(-i\omega, q)d\omega}, \quad (7)$$

$$C_u(i\omega, q) = C(i\omega, q)S(i\omega, q), \quad (8)$$

for the band-limited measurement white noise with the cutoff frequency ω_c . Sensitivity M_n is calculated by using trapezoidal rule for ω_c given with the results of simulation.

The optimal values of parameters q are determined from [2]:

$$q_0 = \arg \min_q \left(\max_{\omega} |Y_d(i\omega, q)| + \lambda_0 \sum_{i=1}^3 \psi_i(\chi_i - \chi_{id}) \right) \quad (9)$$

$$\psi_i(\chi_i - \chi_{id}) = \begin{cases} 0 & \text{for } \chi_i \leq \chi_{id} \\ \chi_i - \chi_{id} & \text{for } \chi_i > \chi_{id} \end{cases} \quad (10)$$

under constraints on the desired sensitivity to measurement noise M_{nd} and desired robustness defined by M_{sd} , M_{Td} . In (9)-(10) the following parameters are used: $\lambda_0=10^{10}$, $\chi_1=M_n$, $\chi_{1d}=M_{nd}$, $\chi_2=M_S$, $\chi_{2d}=M_{sd}$ and $\chi_3=M_T$, $\chi_{3d}=M_{Td}$, where $|Y_d(i\omega, q)|=|G_p(i\omega)S(i\omega, q)/i\omega|$ and $G_p(i\omega)$ is the frequency response of the process. The disturbance following the load step, important for measuring the closed-loop performance [3], is defined by $Y_d(s, q)=G_p(s)S(s, q)/s$. Optimization (1)-(10) is performed by using the particle swarm optimization algorithm [4] for the desired values of M_{nd} , M_{sd} and M_{Td} .

Simulation analyses are performed for stable process $G_{p1}(s)$, integrating process $G_{p2}(s)$ and unstable process $G_{p3}(s)$, in the loop with the PID controller and DTC-PID controller. Process $G_{p1}(s)$ is the model of the laboratory thermal plant, obtained for the nominal regime around the temperature 45°C of the aluminum plate in Fig. 2. Results of simulation analyses are summarized in Tables I-III, Fig.3 and Figs.5-6, for processes defined by the transfer functions

$$G_{p1}(s) = \frac{1.507(3.42s+1)(1-0.816s)}{(577s+1)(18.1s+1)(0.273s+1)(104.6s^2+15s+1)},$$

$$G_{p2}(s) = \frac{1}{s(2s+1)^5}, \quad G_{p3}(s) = \frac{2e^{-5s}}{(10s-1)(2s+1)}.$$

For the same values of M_n , M_S and M_T , and for noise filtering with $n=4$, faster rejection of the load disturbance is obtained with the DTC-PID controller. Besides, and this is of essential importance, the DTC-PID controller performance is characterized with the smooth control signal, lowering wear of active elements in actuator.

TABLE I. PARAMETERS OF THE PID AND DTC-PID FOR G_{p1}

| Controller | k/a_0 | k/a_1 | K_d/a_2 | T_f/T_i | L |
|----------------------|---------|---------|-----------|-----------|-------|
| PID ^a | 0.1312 | 12.6194 | 299.41 | 1.6607 | - |
| DTC-PID ^a | 6.8632 | 638.71 | 9352.5 | 4.9376 | 22.14 |

a. $M_S=1.7$, $M_T=1.3$, $M_n=25$, $\omega_c=2\pi$

TABLE II. PARAMETERS OF THE PID AND DTC-PID FOR G_{p2}

| Controller | k/a_0 | k/a_1 | K_d/a_2 | T_f/T_i | L |
|----------------------|---------|---------|-----------|-----------|------|
| PID ^a | 0.0051 | 0.1225 | 0.7602 | 0.0949 | - |
| DTC-PID ^a | 0.0404 | 0.8243 | 4.4798 | 0.4442 | 3.57 |

a. $M_S=2$, $M_T=1.5$, $M_n=2$, $\omega_c=10\pi$

TABLE III. PARAMETERS OF THE PID AND DTC-PID FOR G_{p3}

| Controller | k/a_0 | k/a_1 | K_d/a_2 | T_f/T_i | L |
|----------------------|---------|---------|-----------|-----------|------|
| PID ^a | 0.0108 | 0.8076 | 3.1940 | 0.1361 | - |
| DTC-PID ^a | 0.0576 | 2.9260 | 10.3595 | 0.4346 | 1.64 |

a. $M_S=3.5$, $M_T=3.5$, $M_n=5$, $\omega_c=10\pi$

III. EXPERIMENTAL ANALYSIS

The temperature $T(x, t)$ of the aluminum plate in Fig.2, long $L=0.1m$ and wide $h=0.03m$, is measured by precision sensors LM35 (TO92) at positions $x=0$ and $x=L$. The controlled variable is $y(t)=T(L, t)$. Measurement at $x=0$ is used to prevent overheating, to keep the temperature $T(0, t) \leq 70^\circ C$ [2]. The plate is heated by the terminal adjustable regulator LM317 (TO 220) at $x=0$. The output of the controller $0 \leq u(t) \leq 100\%$ is the input to the heater.

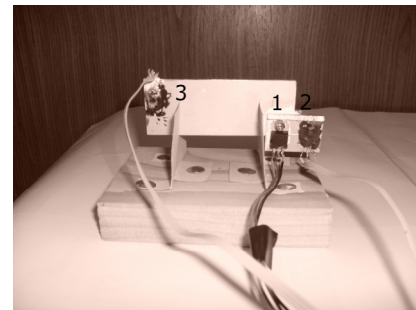


Figure 2. Laboratory thermal plant

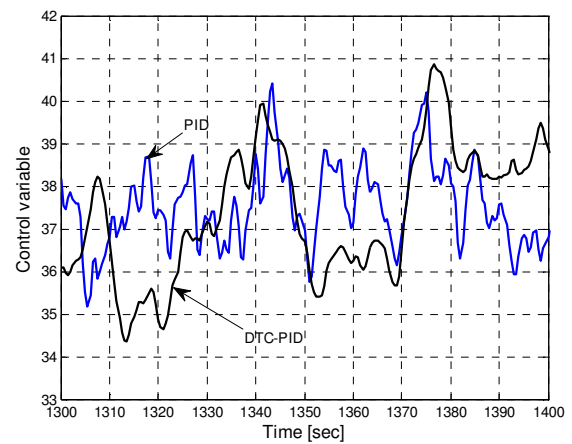
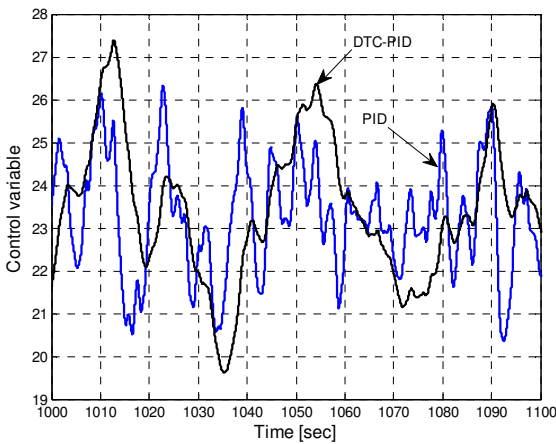
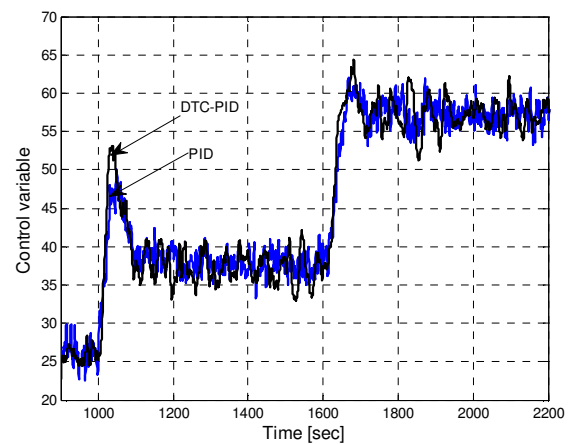
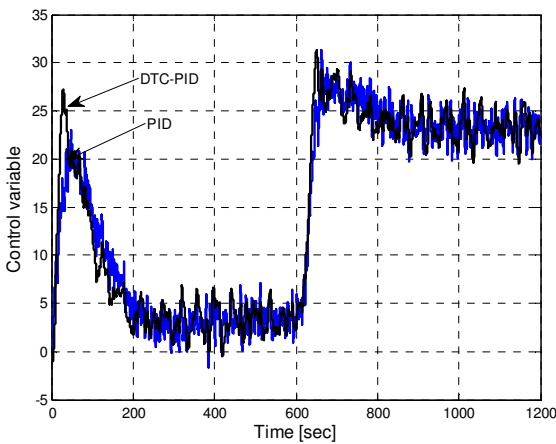
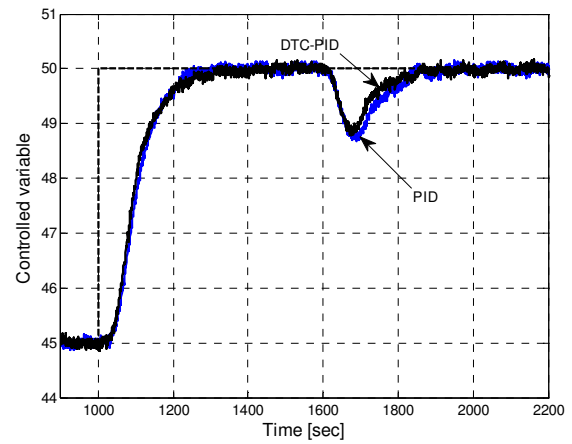
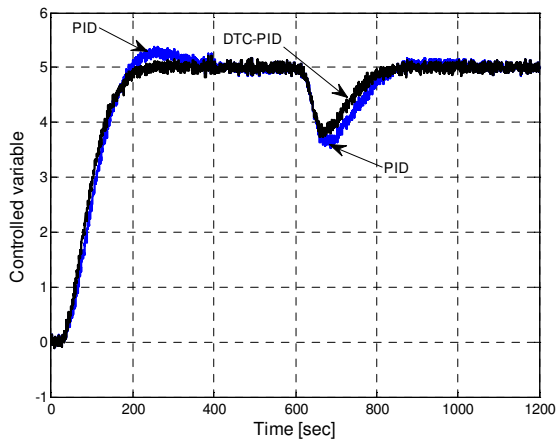


Figure 3. Responses of stable process $G_{p1}(s)$ in the loop with PID and DTC-PID controllers for $n=4$. Set-point $R(s)=5/s$ and load disturbance $D(s)=-20\exp(-600s)/s$. Band-limited white noise with $\sigma^2=0.003$ and $\omega_c=2\pi$ is added to the controlled variable.

Figure 4. Responses of laboratory thermal process in the loop with PID and DTC-PID controllers for $n=4$. Set-point is changed at $t=1000s$ from 45°C to 50°C . A -20% change of the control signal is inserted at $t=1600s$.

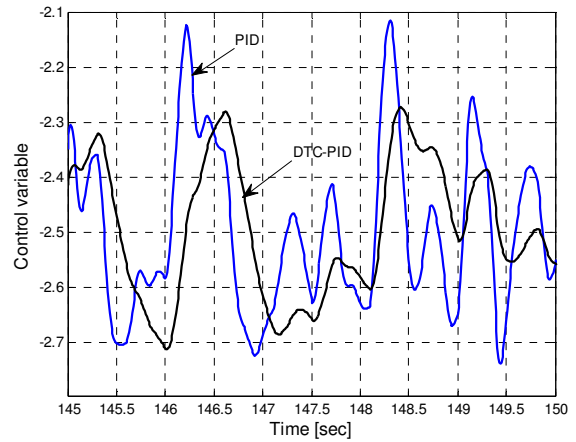
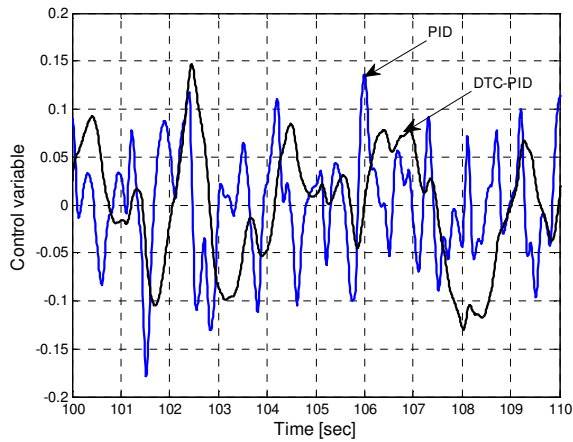
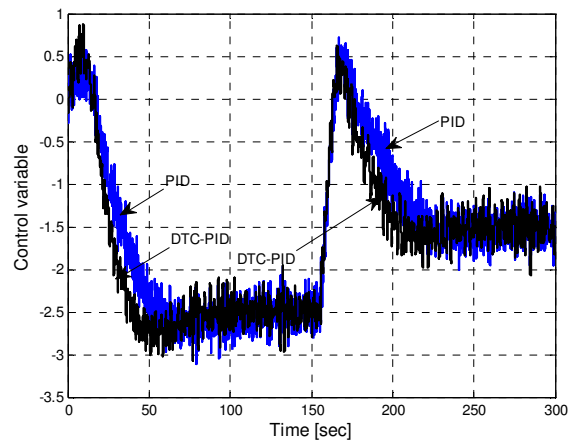
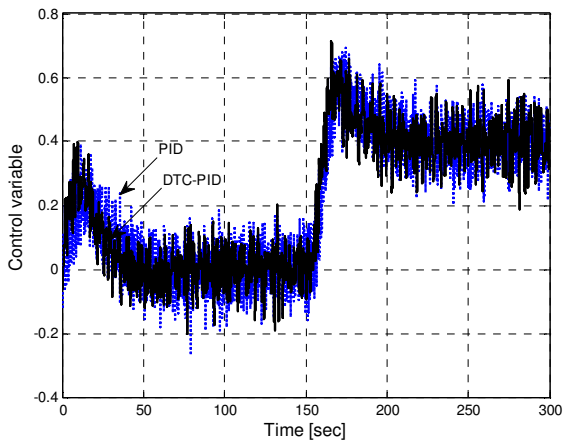
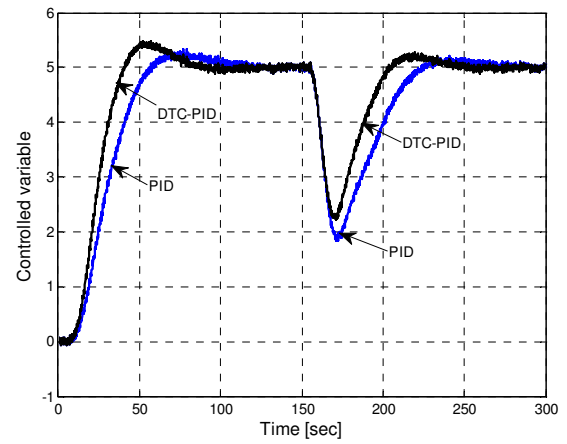
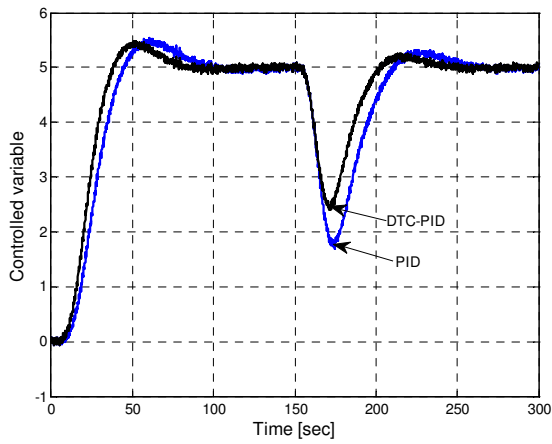


Figure 5. Responses of integrating process $G_{p2}(s)$ in the loop with PID and DTC-PID controllers for $n=4$. Set-point $R(s)=5/s$ and load disturbance $D(s)=-0.4\exp(-150s)/s$. Band-limited white noise with $\sigma^2=0.001$ and $\omega_c=10\pi$ is added to the controlled variable.

Figure 6. Responses of unstable process $G_{p3}(s)$ in the loop with PID and DTC-PID controllers for $n=4$. Set-point $R(s)=5/s$ and load disturbance $D(s)=-\exp(-150s)/s$. Band-limited white noise with $\sigma^2=0.001$ and $\omega_c=10\pi$ is added to the controlled variable.

The frequency response of the laboratory thermal plant model $G_{p1}(s)$ is used to determine parameters of the PID controller and DTC-PID controller, given in Table I. This model is obtained in [2] by determining a 100th order ARX model, reduced than to the 5th order model defined by $G_{p1}(s)$. Responses of the laboratory plant are presented in Fig. 4.

Agreement of the simulation results in Fig. 3 and experimental results in Fig. 4 confirm validity of the model $G_{p1}(s)$. In both analyses, compared to the PID controller, almost the same set-point response and faster rejection of the load step disturbance are obtained by the DTC-PID controller with the smooth control signal.

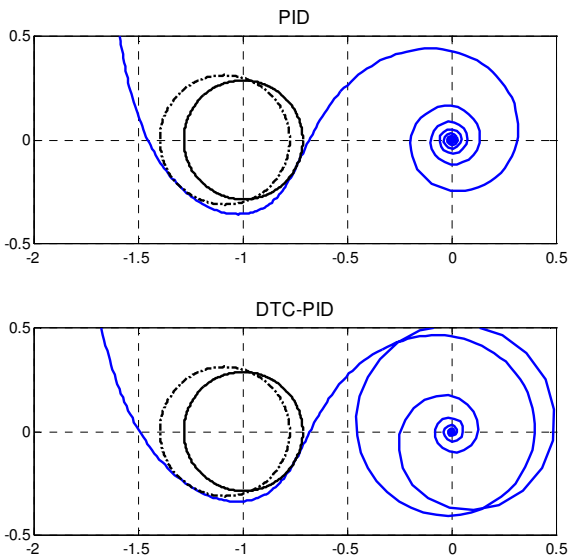


Figure 7. Nyquist curves of the closed-loop systems for $G_{p3}(s)$ in loops with PID and DTC-PID controllers, presented with M_S (solid) and M_T (dashed) circles.

Again, for the higher-order noise filtering, significant improvement of the performance/robustness tradeoff is obtained by the Dead-Time Compensating PID (DTC-PID) controller compared to the PID controller. Namely, as demonstrated in Tables II-III and Figs. 5-6, for the same values of M_n , M_S and M_T , faster set-point responses and faster rejection of the load step disturbance are obtained by the DTC-PID controller. Since the advantages of the DTC-PID controller over recently proposed Dead-Time Compensators is demonstrated in [2], the analysis presented here confirm that the application of the DTC-PID controller is a prerequisite for designing the high-performance control loops at the basic level of the process control. Besides, based on the estimated frequency response of the process in the loop considered, the proposed tuning based on the optimization under constraints on the sensitivity to measurement noise M_n and robustness, defined by the maximum sensitivity M_S and maximum complementary sensitivity M_T , is effective. This is clearly confirmed by the Nyquist diagrams presented in Fig. 7 for the unstable process $G_{p3}(s)$ in the loop with the PID and DTC-PID controllers, tuned as defined in Table III. For further details related to the optimization of the DTC-PID controller see [2, Appendix B].

IV. CONCLUSION

The high performance/robustness tradeoff of the DTC-PID controller, demonstrated in [2], is preserved also when the fourth-order noise filter is applied. Compared to the PID controller with higher-order noise, the significant reduction of the variation of the control signal in the presence of the measurement noise is obtained by the DTC-PID controller, preserving the performance measured by the set-point and load disturbance step responses. This effect can be explained as follows.

To reduce the control signal variation, the higher-order noise filtering must be applied. However, in this case an additional lag is inserted in the loop. As a consequence, reduction of the noise filter time constant T_f is obtained in the PID controller optimization. In the DTC-PID controller optimization, this additional lag is naturally compensated by the dead-time compensating loop in Fig.1. Thus, for the same values of the desired sensitivity to measurement noise M_{nd} , and desired robustness indices M_{Sd} and M_{Td} , the high performance is obtained by applying DTC-PID controller with the smooth control signal.

ACKNOWLEDGMENT

Aleksandar Ribić acknowledges the financial support from Serbian Ministry of Science and Technology (Project TR33022 and TR35003).

REFERENCES

- [1] M.R. Mataušek, T.B. Šekara, PID controller frequency-domain tuning for stable, integrating and unstable processes, including dead-time, *J. Process Control*, vol 21, pp. 17-27, 2011.
- [2] A. I. Ribić, M. R. Mataušek, Dead-time compensating PID controller, *J. Process Control*, vol. 22, pp. 1340-1349, 2012.
- [3] F.G. Shinskey, How good are our controllers in absolute performance and robustness?, *Measurement and Control*, vol. 23, pp. 114-121, 1990.
- [4] M.R. Rapaić, Matlab implementation of the Particle Swarm Optimization (PSO) algorithm, <http://www.mathworks.com/matlabcentral/fileexchange/22228-particleswarm-optimization-pso-algorithm>